RELATIVELY LOW POROSITIES DETECTED WITHIN LUNAR FARSIDE BASINS. T. K. Venkatadri[1] and P. B. James[2,3], [1]Ardsley High School, 300 Farm Road, Ardsley, NY 10502 (tara.venkatadri@gmail.com), [2]Lunar and Planetary Institute, Houston, TX 77058, [3]Baylor University Department of Geosciences, Waco, TX 76798.

Introduction: The lunar farside highlands have reached a state of crater saturation, and approaches besides crater counting must therefore be explored to determine the cratering history of the highlands. Understanding the relationships between lunar impact events and porosity can help to infer the frequency and size of impact events during the formation of the solar system.

Porosity signatures in impact basins result from a combination of two effects: the compaction of porous target materials and the generation of new porosity via rock fracturing. Based on the relative porosity calculated in and around a basin, it is possible to determine which effect is stronger.

Previous studies have explored porosity variations in the lunar crust over differently sized areas. On a large scale (12° of latitude and longitude), significant amounts of porosity (12%) were found to extend into the mantle [1]. An analysis of residual Bouguer gravity indicated that porosity increases in lunar bowl-shaped craters (diameter < 200 km) [2].

Despite the studies of porosity in smaller basins, higher-resolution porosity variations in larger basins have not yet been explored. Rock bulk density was calculated through a least-squares fit between GRAIL gravity and LOLA gravity-from-topography [3] and used to estimate rock porosity in the Hertzsprung, Freundlich-Sharonov and Korolev basins. Porosity values were calculated for every 2° x 2° region within these basins. This study uses a ratio between gravity and gravity-from-topography rather than spectral analysis to observe high-resolution porosity variations in impact basins.

Methods:

Mapping Bulk Density in Large Farside Basins.

Free air gravity was calculated using the GRGM1200A GRAIL gravity model at a reference radius of 1744 km. The gravity data were filtered between spherical harmonic degrees 100 and 700 to be primarily sensitive to shallow crustal density, and the filtered gravity field was evaluated on a grid with 0.1º spacing in both latitude and longitude. A similar grid of gravity-from-topography of unit density was generated using a finite-amplitude calculation with LOLA topography coefficients [4].

The Hertzsprung, Freundlich-Sharonov (F-S), and Korolev basins (Table 1) were chosen based on their size (430-600 km, larger than previously studied basins and too small to be resolved by spatio-spectral localization) and their proximity to the Equator [5, 6]. The bulk density of the rock in each basin was calculated as the ratio of gravity to gravity resulting from topography of unit density every 2° x 2° within and around the basins (up to 120 km away from the basin rim).

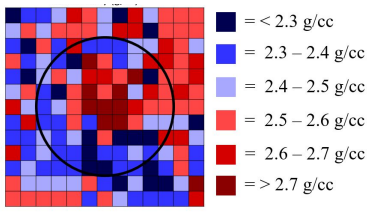

Figure 1: Bulk density in the Hertzsprung basin as calculated using the correlation between gravity and gravity-from-topography. The scale used in coloring the map is shown on the right.

Basin	Basin Location	Comparison Region Location
Hertzsprung	14.3ºN - 11.6ºS, 218.3ºE - 244.2ºE	26.0ºN - 0.1ºN, 190.0ºE - 213.9ºE
F-S	33.0ºN - 5.1ºN, 162.0ºE - 189.9ºE	16ºN - 11.9ºS, 122.0ºE - 149.9ºE
Korolev	8ºN - 15.9ºS, 190.6ºE - 214.5ºE	18.0ºN - 5.9ºS, 216.0ºE - 239.9ºE

Table 1. Locations of basins and comparison regions

Accounting for Grain Density and Elevation.

Figure 1 depicts Hertzsprung basin bulk density. It was necessary to correct these density values to reflect only the density variations arising from porosity variations because not all changes in bulk density can be attributed to porosity. Compositional variations can lead to changes in grain density (i.e. the density of a non-porous rock), and gravity studies of higher-elevation terrain tend to yield artificially low bulk density values due to a greater sensitivity to the near-surface porosity gradient [7].

A comparison region relatively devoid of large basins was selected for each basin based on similarities in topography and iron content (Table 1). The density of each 2° x 2° area within these regions was calculated. Least-squares fits were performed between density and topography and density and FeO for each comparison region using the calculated bulk density and Clementine topography and FeO values

[8]. It was concluded that density decreases by 0.032 g/cc as topography increases by 1 km from the average of the slopes of the lines of best fit for the density-topography correlations. It was also concluded that density increases by 0.009 g/cc for each increase of 1 wt% FeO by averaging the slopes for the density–FeO correlations.

These values were used to correct the density values so that each density value represented rock with 0 wt% FeO at 4 km elevation. This correction did not take any possible correlation between FeO and topography into account, assuming that these factors would be independent of one another. The grain density of pure anorthosite (a rock type with no FeO), 2.75 g/cc [7], was used to estimate the porosity in each region using the equation $\rho = \rho_{grain} \cdot (1 - \varphi)$, where ρ was the corrected bulk density estimate, ρ_{grain} was the grain density of pure anorthosite, and φ was the porosity. A t-test was used to determine the statistical significance of the difference in porosity in the basin rims and interiors.

Results:

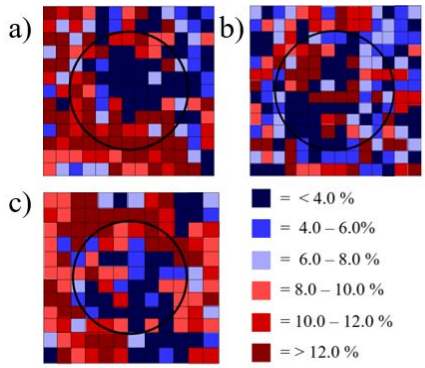

Figure 2: Porosity in the interior and rim of the (a) Hertzsprung, (b) F-S, and (c) Korolev basins.

Basin	Mean φ in Basin Interior	Mean φ in Basin Rim	P-Value
Hertzsprung	6.34 %	8.98 %	0.0109 *
F-S	6.52 %	6.63 %	0.9122
Korolev	5.95 %	8.95 %	0.0037 *

Table 2. Mean porosity (φ) and p-values from unpaired t-test for each basin's interior and rim porosity. * = p <0.05

Figure 2 shows maps of porosity in the three basins, and Table 2 shows the statistical significance of the porosity difference between each basin interior and rim. The porosity variations due to cratering are best defined in the Nectarian-age Hertzsprung basin (Figure 2a), where the porosity significantly decreases in the center of the basin and increases towards the rim. Porosity variations in the Freundlich-Sharonov basin (Figure 2b) are less defined and do not show a statistical significance. This may be due to the basin's pre-Nectarian age or the elimination of the basin's porosity signature via superimposed cratering. However, the areas of lowest porosity were still found within the basin, so a correlation may exist that was not observed using the techniques described in this study. The Nectarian-age, ringed Korolev basin (Figure 2c) has its lowest porosity just east of the center, where there is known to be a terrace. This terrace may have formed from the excavation of low-porosity rock from deeper within the crust, resulting in the observed decrease in porosity. The Korolev basin, like the Hertzsprung basin, shows a significant decrease in porosity from the rim to the interior.

In these basins, porosity tended to be lowest near the center of the basin, and two of the three basins showed a statistically significant decrease in porosity from the basin interior to the rim. Because the final porosity of any cratered region on the Moon depends on the interaction between compaction and fracturing, the observed porosity signature indicates which force overcomes the other. Based on data of these basins, compaction associated with the basin-forming impact overrides the effect of fracturing, decreasing crustal porosity in Nectarian-age highlands basins 430 to 600 km in diameter.

This trend in porosity is interesting since it is opposite of the trend Soderblom et al. (2015) observed in smaller craters, where fracturing predominated over compaction [2]. Further investigation may determine if larger-size impact events create stronger compacting forces than fracturing forces or if basin type [9] affects porosity.

An increased knowledge of lunar porosity will enable the understanding of ancient geologic processes on the Moon and, by extension, on Earth. The causes, properties, and effects of these processes may be determined in the future using models that incorporate the findings of this study.

References: [1] M.A. Wieczorek et al. (2013) *Science* 339, 671-675. [2] J.M. Soderblom et al. (2015) *GRL* 42. [3] M.T. Zuber et al. (2013) *Science* 339, 668-671. [4] Wieczorek M. A. and Phillips R. J. (1998) *JGR* 103*, 1715-1724*. [5] P.G. Lucey et al. (2014) *American Mineralogist* 99, 2251-2257. [6] K. Miljković et al. (2014) *Earth and Planetary Science Letters* 409, 243-251. [7] J. Besserer et al. (2014) *GRL* 41, 5771-5777. [8] J.J. Gillis et al. (2004) *Geochimica et Cosmochimica Acta* 68, 3791-3805. [9] G.A. Neumann et al. (2015) *Science Advances* 1, 9.